Physica A 593 (2022) 126979

Contents lists available at ScienceDirect

Physica A

journal homepage: www.elsevier.com/locate/physa

Population density impact on COVID-19 mortality rate: A multifractal analysis using French data

R. Pascoal [a], H. Rocha [a,b,*]

[a] CeBER, FEUC, Univ. Coimbra, Av. Dias da Silva 165, 3004–512 Coimbra, Portugal
[b] INESC-Coimbra, Rua Sílvio Lima, Polo II, 3030–290 Coimbra, Portugal

ARTICLE INFO

Article history:
Received 26 July 2021
Received in revised form 6 January 2022
Available online 29 January 2022

Keywords:
COVID-19
France
Population density
Multifractal analysis

ABSTRACT

The current COVID-19 pandemic caught everyone off guard and is an excellent case study to investigate the real impact of population density on emerging highly contagious infectious diseases. The relationship between the threat of COVID-19 and population density has been widely debated not only in scientific articles, but also in magazines and reports around the world. It appeared both in the columns of experts and in the speeches of politicians, yet without reaching any consensus. In this study, using COVID-19 data from France, we try to shed light on this debate. An alternative density measure, weighted by population, is used. This novel density measure clearly outperforms the commonly used density in terms of relationship with COVID-19 deaths and proved to be competitive with some of the best known predictors, including population. A multifractal analysis, characterizing different space distributions of population in France, is used to further understand the relation between density and COVID-19 mortality rate.

1. Introduction

The current COVID-19 pandemic caught everyone off guard and quickly spread to the four corners of the world after it was first reported in Wuhan, China, in the end of 2019. France was the first European country with reported cases of COVID-19 that dates back to January 24, 2020 [1]. Since then, the number of cases and the number of deaths have grown, systematically placing France in the world's top ten in these two parameters.

The dynamics of virus propagation and mortality over time depends on several factors including more or less restrictive measures on population movement. One of the most effective measures used by different governments in the beginning of COVID-19 pandemic, but also one of the most restrictive, is the lockdown with a mandatory home confinement except for a short list of essential activities. In France, the lockdown took place on March 17, 2020, decisively helping to control a first wave of COVID-19 cases and deaths, as illustrated in Fig. 1.

The relationship between the threat of COVID-19 and population density has been widely debated not only in scientific articles, but also in magazines and reports around the world. It appeared both in the columns of experts and in the speeches of politicians, yet without reaching any consensus [2–6]. Due to the pandemic characteristic of COVID-19, i.e. the fact that it spreads through physical contact between people, a natural explanation for the dynamics of the number of COVID-19 cases and resulting deaths is the degree of concentration of individuals in space. The diverging evolution of these dynamics among regions can, in principle, be explained by differing patterns of population distribution. However, many studies in different countries contradict this theory and claim that population density – the number of people per square

* Corresponding author at: CeBER, FEUC, Univ. Coimbra, Av. Dias da Silva 165, 3004–512 Coimbra, Portugal.
E-mail addresses: ruiapsp@fe.uc.pt (R. Pascoal), hrocha@fe.uc.pt (H. Rocha).

https://doi.org/10.1016/j.physa.2022.126979
0378-4371/

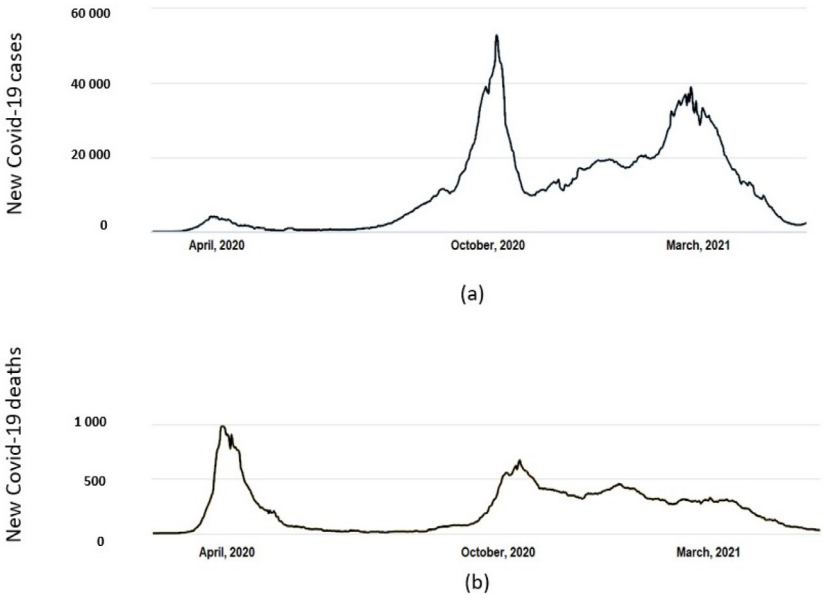

Fig. 1. Seven-day moving average of novel daily cases of COVID-19 in France (a) and seven-day moving average of novel daily deaths of COVID-19 in France (b).

kilometer – had no significant relationship with infection and mortality rates [3–6]. E.g., Hamidi, a public-health expert at Johns Hopkins, and her collaborators at the University of Utah studied the impact of density on the COVID-19 infection and mortality rates for 913 U.S. metropolitan counties [3]. The Johns Hopkins — Utah study found that metropolitan population is one of the most significant predictors of infection rates while county density had no significant relationship with infection rate. Furthermore, counties with higher densities have significantly lower virus-related mortality rates than do counties with lower densities [3]. This statement implies a paradoxical relationship that we aim to debate in this work. The generalization that high-density population means lower virus-related mortality should not be made lightly due to the multifactorial nature of COVID-19 and the interaction between the different factors.

In this study we try to shed light on whether the link between population density and the threat of COVID-19 (or future emerging highly contagious infectious diseases) is a myth or not, and whether this predictor should play a role in epidemiological models. To that end, using COVID-19 data from France, the relationship between density (and also population) and the number of deaths from COVID-19 is studied. The choice of mortality data is due to the fact that this type of data is apparently more reliable and less dependent on local testing strategies than confirmed cases of COVID-19 [7,8]. An alternative density measure, weighted by population, is used. This novel density measure clearly outperforms the commonly used density in terms of relationship with COVID-19 deaths and proved to be competitive with some of the best known predictors, including population. In fact, considering the density measure proposed here, there is a clear improvement in R^2 compared to the regression using the usual density. A multifractal analysis, characterizing different space distributions of population in France [9], is used to further understand the relation between density and COVID-19 mortality rate. This multifractal analysis allows (i) to identify five different types of space distributions of population in France, (ii) to distinguish groups of subregions (“départements") with different types of predominant space distributions of population, and (iii) to identify subgroups in the scatter plot with different regression for each subgroup of observations (sub-regions). One of the advantages of this approach is therefore to allow detailing the analysis carried out in other articles where only one regression for all observations is considered [3–6].

2. Materials and methods

2.1. Data

Mainland France is organized in 13 regions (Fig. 2(a)) and 96 counties called “départements" (Fig. 2(b)). For this study, we obtained from Santé Publique France, the number of COVID-19 hospital deaths, excluding nursing homes, by county in mainland France, from the beginning of this pandemic until the end of 2020 [10]. Vaccination in France against COVID-19 started in the beginning of 2021 which could add an additional bias to this study. Area and estimated population of each French county in the 1st of January, 2021 was provided by INSEE (L’Institut National de la Statistique et des Études Économiques) [11].

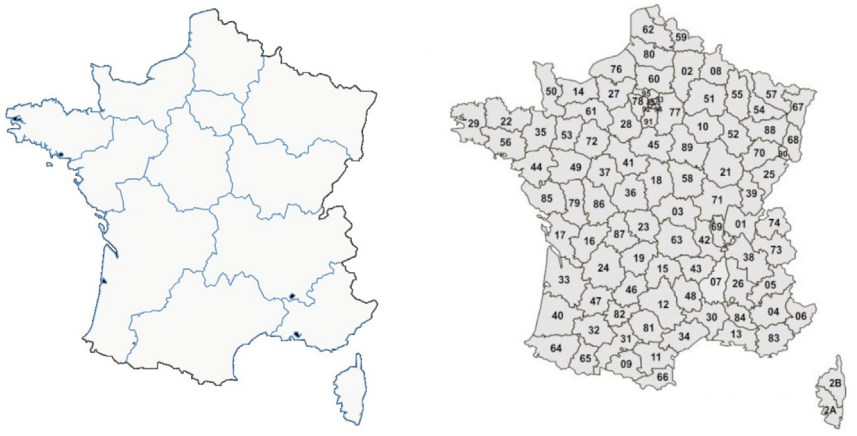

(a) (b)

Fig. 2. Regions in mainland France, including Corsica island, (Fig. 2(a)) and corresponding départements (counties) (Fig. 2(b)).

2.2. Statistical framework

The most simple form to address the degree of population concentration in a region is to assume homogeneity in its distribution in space. In this simplified context, the classical definition of population density given by $D = \frac{P}{A}$, where P is total population of the region and A is the corresponding area, is the concept that intuitively surfaces as a concentration measure. It follows that a relation can be found between the number of deaths resulting from COVID-19 (DT) and density (D) given by

$$DT = aD^b,$$

where a is a scaling parameter and b represents the elasticity of DT with respect to D.

This relation is based on the argument that presents physical distance between people as a cause for the probability of being contaminated. The formalization of this link between density and the potential for contact of an individual with another individual is made by Pan et al. [12]. Further analyses on the relation between events related to pandemics and density were made by Cardoso and Gonçalves [13], Li et al. [14] and Hu et al. [15].

As claimed before, the classical definition of density is well suited for the case where the assumption of spatial homogeneity is a good approximation. Let us now consider a modified definition of density that allows some spatial heterogeneity. The modified version of density that we consider is known as population-weighted density [16]. The context where this definition acquires relevance is the one where a region is divided into n subregions having distinct population and area. Let region i have population p_i, area a_i and, consequently, density $d_i = \frac{p_i}{a_i}$. Then, the classical density becomes:

$$D = \frac{P}{A} = \frac{\sum_{i=1}^{n} p_i}{\sum_{i=1}^{n} a_i} = \frac{\sum_{i=1}^{n} a_i \frac{p_i}{a_i}}{\sum_{i=1}^{n} a_i} = \frac{\sum_{i=1}^{n} a_i d_i}{\sum_{i=1}^{n} a_i}.$$

Thus, the classical region density can be seen as the average of the subregions densities where each one of these is weighted by the corresponding area. It is therefore an area-weighted density. On the other hand, the modified density is population-weighted:

$$D^* = \frac{\sum_{i=1}^{n} p_i d_i}{\sum_{i=1}^{n} p_i}. \tag{1}$$

In this study, we claim that it may be valuable to consider a relation between DT and D^* (instead of D):

$$DT = a(D^*)^b.$$

Fig. 3 aims to illustrate the reasoning for admitting advantages in considering a population-weighted density. In Fig. 3 we have two regions, R_1 and R_2, where it is visible that there is more homogeneity in R_2 than in R_1, which reflects in a smaller difference between the subregions in terms of population distribution. Assuming that there is a critical distance between individuals below which the risk of contamination becomes more effective, then it is likely that the risk of contagion for the first subregion of R_1 is higher than in all other subregions.

The increased risk highlighted in Fig. 3 for a single subregion can be spread to the whole region, accounting for the fact that physical distance is not an absolute barrier: a single individual moving from one subregion to another is enough

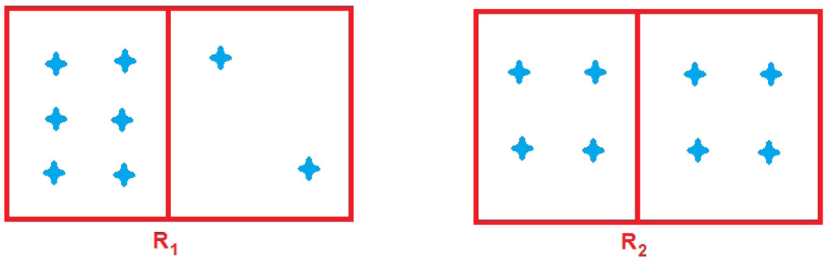

Fig. 3. Illustration of possible advantages in considering a population-weighted density.

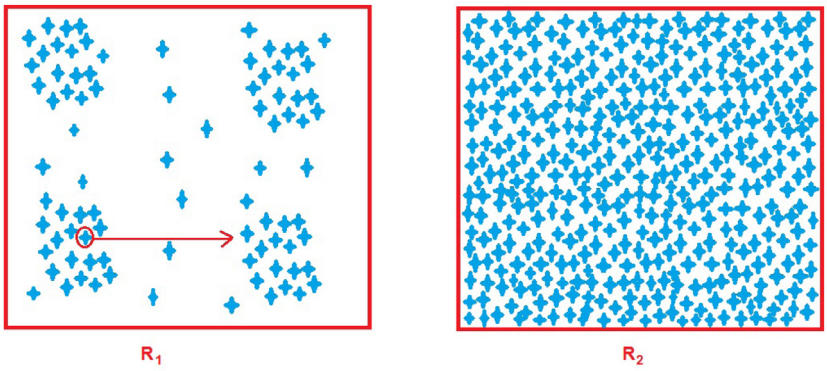

Fig. 4. Illustration of dissemination risk similarity between a "dense region" (R_1) and a "big city" (R_2).

to spark a new source of contagion, as illustrated in region R_1 of Fig. 4. In that sense, a "big city" with a very large density, including vertical growth at the level of skyscraper, may not constitute much higher risk than regions having lower density spread in some localized focus with intermediary zones relatively populated (see Fig. 4). Percolation is a line of research that could fruitfully explore this aspect [17], just as is done in studying the dynamics of forest fire: a spark flying from one section of the forest to another can initiate a replica there with the power to fully consume it. Regardless of the interest of this possible line of investigation, as observed for the subregions in Fig. 3, in Fig. 4 it is likely that the risk of contagion in R_2 is higher than in R_1. Thus, generalizations should not be made lightly as previously remarked.

The recognition that such an analysis is based on a mean measure (density) defined on physical entities (regions) for a particular scale and that different scales may lead to distinct results leads naturally to the introduction of the concept of fractal. Multifractal analysis has been used in epidemiological models to characterize and understand the incidence of infection time series [18] and recently in COVID-19 studies [19,20].

2.3. Multifractal analysis

A fractal system is one which is characterized by a scaling relation

$$D(a) \sim a^H,$$

where D is a given quantity, H is a fractal exponent and a is a scale parameter (see, e.g., [21]). We consider a unit of area, a, that can be made arbitrarily small and D is the density corresponding to a cell with area a. The advantage of this approach is that the scaling relationship does not depend on scale. The density is measured at each point considering the limit as a tends to zero. Thus, we have local densities. The concept of fractal is intimately linked to the one of self similarity: it is assumed that the pattern is repeated in different scales.

When there is a single scaling relation at each point, that is we have a monofractal, the underlying representation of population distribution is relatively homogeneous; it is assumed that there are identical buildings with a similar distribution is space where the exponent influences the concentration degree between buildings (see Sémécurbe et al. [9]). For other applications of multifractal on urban population distribution see also Chen and Wang [22] and Frankhauser [23].

The concept of fractal can be generalized to the one of multifractal. A multifractal system is one characterized by scaling relations with different exponents in infinite number [21]. The distinction with respect to monofractal is that the later implies a binary analysis, i.e., at each point the event may or may not occur (e.g., existence of buildings), whereas in multifractal, the relative amount of the event is considered and the intensity of occurrence depends on the spatial space [9]. There is diversity of building patterns in space including houses of several sizes, huge collective buildings, etc.

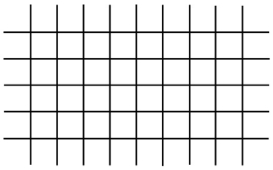

Fig. 5. Illustration of a grid of square cells with side length r.

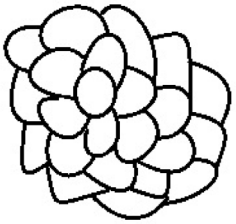

Fig. 6. Illustration of a grid of cells with nonuniform frontier.

To start a more technical description of multifractal, consider the concept of multifractal measure [24]. Let D be a space. A multifractal measure, μ, on D is a measure such that:

(a) For any $x \in D$, $\mu_r(x) \sim r^{\alpha_x}$ where r is the radius of a ball around x and the stated relation holds for r small; thus, $\alpha_x = \lim_{r\to 0} \frac{\log \mu_r(x)}{\log r}$, which is called a singularity strength;

(b) For all α, the set of points with a scaling exponent α is a monofractal having fractal dimension $f(\alpha)$, as measured for instance by the box-counting dimension or the Hausdorff dimension.

Let $N_r(\alpha)$ be the measurement referred in b), then $N_r(\alpha) \sim r^{-f(\alpha)}$ and the function $f(\alpha)$ is called the multifractal spectrum. The characterization of the multifractal can be made through the plot of $f(\alpha)$ on α. To define box-counting dimension, well suited for spatial data, a grid of square cells is defined each with side length r, as illustrated in Fig. 5. Let S be a set of points of the plane. The box-counting of S is given by $\lim_{r\to 0} \frac{\log N_r(S)}{-\log r}$, where $N_r(S)$ is the number of cells that intersect S. This was the dimension considered by Sémécurbe et al. [9]. The Hausdorff dimension allows to adjust to irregular sets, considering cells of nonuniform frontier, as illustrated in Fig. 6 but is difficult to apply.

A partition function, $Z(q)$, is given by $Z(q) = \sum_i \mu_i^q(r) \sim r^{\tau(q)}$, where the sum is over all cells i in the grid and $\tau(q) = \lim_{r\to 0} \frac{\log \sum_i \mu_i^q(r)}{\log r}$ is the Rényi exponent. This function is such that for each q there is an α that mostly contribute to this measure, and which minimizes $\tau(q) = \alpha q - f(\alpha)$. By Legendre transform,

$$\alpha(q) = \tau'(q),$$

$$f(\alpha(q)) = \alpha q - \tau(q).$$

This allows to estimate the multifractal spectrum after $\tau(q)$. Remark that this expressions can be expressed in terms of the generalized dimensions:

$$D(q) = \begin{cases} \frac{\tau(q)}{1-q} & , \text{if } q \neq 1 \\ \lim_{r\to 0} \sum_{i:\mu_i(r)>0} \mu_i(r) \log \mu_i(r) & , \text{if } q = 1. \end{cases}$$

Given the instability of the Legendre transform based estimator, Sémécurbe et al. [9] use the formula of Chhabra and Jensen [25] to estimate the multifractal spectrum. They consider 200 meters side length cells for the French territory, at the more fine resolution. Taking the regression over a set of scales, multifractal spectrum is estimated for each of the spatial units with 25 km of side length over which the French territory is partitioned. Remark that the limits which define singularity strength and spectrum are estimated by regressions of the log measure on the logscale for small enough scales.

Hierarchical cluster analysis based on Hausdorff distances between multifractal spectra allowed Sémécurbe et al. to define a typology of five main types of regions that characterize different space distributions of population in France [9]. The five classes identified after a dendrogram were: the first two are areas of villages or small towns with scarce population around (with the first class less locally concentrated than the second); the third is constituted by peripheries of big cities or rural regions; the fourth is located in great urban centers and the fifth corresponds mostly to villages in areas of low uniform density. The map with the distribution of these classes in the French territory is displayed in Fig. 7.

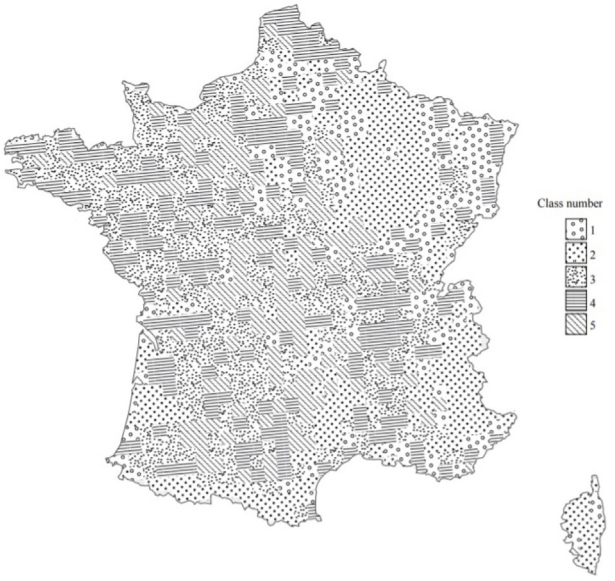

Fig. 7. Map of the distribution of five main types of regions that characterize different space distributions of population in France according to multifractal analysis [9].

3. Results

The relations between population and density with COVID-19 mortality rate were first estimated, in a linearized form, for all counties in mainland France. Figs. 8(a) and 8(b) depict these relations and, as expected, increased population or density correspond to increased mortality rates. It can be seen that there is a better adjustment considering the population. In fact, for regions with large cities and higher densities, the difficulty of adjustment is more visible in the case of density (see points farther to the right in Fig. 8(b)).

Calculation of an adjusted density requires a further refinement of the French map grid. Each of the 96 French counties (départements) considered is organized in many "communes" totaling around 30,000. Population and area of each "commune" was provided by INSEE [11] allowing the calculation of the adjusted density using Eq. (1). Fig. 8(c) depict the relation between adjusted density and COVID-19 mortality rate, in a linearized form, showing a better adjustment of the straight line to the points. The distribution of points which moved horizontally seems more uniform, being remarkable that the points on the right, containing big cities, are now closer to the straight line.

The multifractal analysis we made has as a starting point the French map of Fig. 7, which depicts the five main types of regions that characterize different space distributions of population in France [9]. For each of the 96 counties, the predominant class was identified, allowing to distinguish the points that belong to each class in Fig. 9. Considering the regression line that includes all points (counties) the most prominent findings that are a common denominator in the three cases are: most of the points in class 1 are above the regression line but not so much those of class 2, which means that for less strong urban concentration the lethality was increased; points in classes 3 and 5 are mostly below the regression line which seems to underline the advantage of this pattern of rural or suburban spatial distribution; in class 4 (urban pattern) the evidence is mixed, but for the 3 most dense urban departments the deaths are below the regression line.

In Fig. 9, the relations between population, density and adjusted density with COVID-19 mortality rate were also estimated, in a linearized form, for the five colored subgroups of counties. R^2 values for regressions considering all counties in mainland France are depicted as well as R^2 values for regressions considering the five colored subgroups of counties. Two types of information can be extracted from these values: on one hand, comparing the different predictors when using all observations and, on the other hand, figuring out which subgroup(s) of counties fit worst. For population and adjusted density slopes are very similar except for class 2 while slopes differ substantially for density. Interestingly, mortality rate is best explained by population ($R^2 = 0.844$) and density (0.851) for class 1 counties while for adjusted density is best explained for class 4 ($R^2 = 0.74$). Both density and adjusted density presented the most difficulties for class 2 counties while population performs worst for urban pattern (class 4).

4. Discussion and conclusion

The current COVID-19 pandemic has attracted the interest of the academic community, giving rise to a growing number of studies on this topic [26–34]. One of the topics that has raised many discussions is the impact of density on this

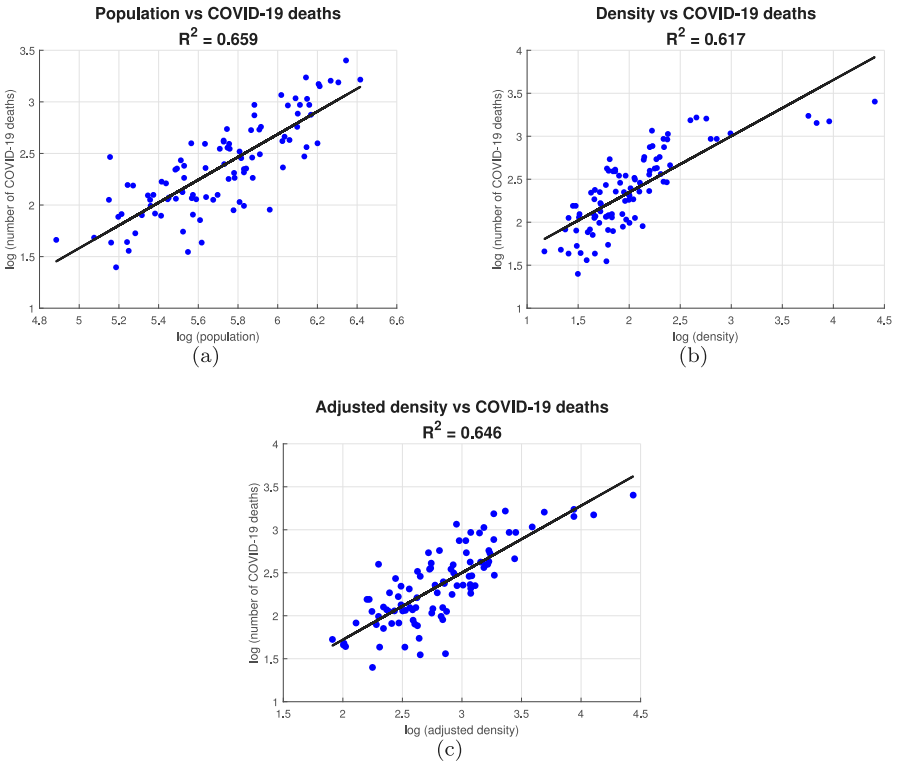

Fig. 8. Relations between population, density and adjusted density with COVID-19 mortality rate, in a linearized form (log–log regression), for all counties in mainland France.

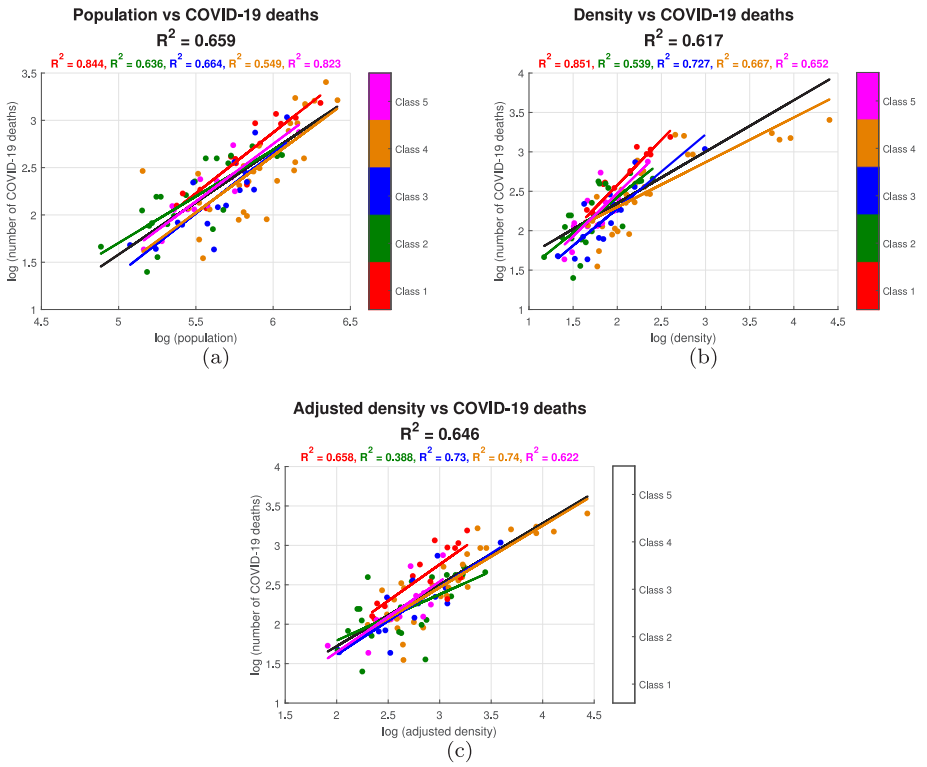

Fig. 9. Relations between population, density and adjusted density with COVID-19 mortality rate, in a linearized form (log–log regression), stratified by type of regions.

pandemic. In this study, using data from France, we compared the relation of population and density with COVID-19 mortality rates. The relation between an adjusted density and the chosen outcome was also proposed, clearly improving the fitting when compared to density.

A multifractal analysis was also performed, allowing to differentiate the behavior of the different features (population, density and adjusted density) for the five main types of regions that characterize different space distributions of population in France. This multifractal analysis led to very interesting results such as the fact that most counties with small villages or towns and with scarce population around (class 1) presented increased COVID-19 lethality as opposed to the three most dense urban counties (class 4) that presented a decreased number of COVID-19 deaths. Different factors have certainly contributed for these findings, including the existence of more health infrastructures in the more concentrated regions which allow for more efficient answers to pandemics, particularly in early days when this pandemic deaths curve reached its peak.

An overall conclusion that can be drawn from this study is that density should be considered in the different epidemiological models as it contains complementary information to population size. However, considering density at a "microscopic" level can be more informative than the "macroscopic" density considered in most of the studies.

CRediT authorship contribution statement

R. Pascoal: Main research, Brainstorming, Writing the manuscript, Manuscript revision. **H. Rocha:** Main research, Brainstorming, Writing the manuscript, Manuscript revision.

Declaration of competing interest

The authors declare that they have no known competing financial interests or personal relationships that could have appeared to influence the work reported in this paper.

Acknowledgments

This study has been funded by national funds, through FCT, Portuguese Science Foundation, under project UIDB/05037/2020. All authors approved the version of the manuscript to be published.

References

[1] S.B. Stoecklin, P. Rolland, Y. Silue, A. Mailles, C. Campese, A. Simondon, M. Mechain, L. Meurice, M. Nguyen, C. Bassi, E. Yamani, S. Behillil, S. Ismael, D. Nguyen, D. Malvy, F.X. Lescure, S. Georges, C. Lazarus, A. Tabai, M. Stempfelet, V. Enouf, B. Coignard, D. Levy-Bruhl, I. Team, First cases of coronavirus disease 2019 (COVID-19) in France: surveillance, investigations and control measures, January 2020, Eurosurveillance 25 (2020) 2000094, http://dx.doi.org/10.2807/1560-7917.

[2] D.W.S. Wong, Y. Li, Spreading of COVID-19: Density matters, PLoS One 15 (2020) e0242398, http://dx.doi.org/10.1371/journal.pone.0242398.

[3] S. Hamidi, S. Sabouri, R. Ewing, Does density aggravate the COVID-19 pandemic? J. Am. Plan. Assoc. 86 (2020) 495–509, http://dx.doi.org/10.1080/01944363.2020.1777891.

[4] W. Fang, S. Wahba, Urban density is not an enemy in the coronavirus fight: Evidence from China, 2020, World Bank, https://blogs.worldbank.org/sustainablecities/urban-density-not-enemy-coronavirus-fight-evidence-china.

[5] J. Hsu, Population density does not doom cities to pandemic dangers, scientific American, 2020, https://www.scientificamerican.com/article/population-density-does-not-doom-cities-to-pandemic-dangers/.

[6] J. Davidson, COVID-19 data reveal that urban density is not the enemy, intelligencer, 2020, https://nymag.com/intelligencer/2020/08/covid-19-studies-are-proving-that-density-is-not-the-enemy.html.

[7] A.L. García-Basteiro, C. Chaccour, C. Guinovart, A. Llupià, J. Brew, A. Trilla, A. Plasencia, Monitoring the COVID-19 epidemic in the context of widespread local transmission, Lancet Respir. Med. 8 (2020) 440–442, http://dx.doi.org/10.1016/S2213-2600(20)30162-4.

[8] L. Roques, O. Bonnefon, V. Baudrot, S. Soubeyrand, H. Berestycki, A parsimonious approach for spatial transmission and heterogeneity in the COVID-19 propagation, R. Soc. Open Sci. (2020) http://dx.doi.org/10.1098/rsos.201382.

[9] F. Sémécurbe, C. Tannier, S.G. Roux, Spatial distribution of human population in France: exploring the modifiable areal unit problem using multifractal analysis, Geograph. Anal. 48 (2016) 292–313, http://dx.doi.org/10.1111/gean.12099.

[10] Santé publique France, 2021, https://www.santepubliquefrance.fr/dossiers/coronavirus-covid-19/. (Accessed 19 July 2021).

[11] INSEE, https://www.insee.fr/. (Accessed 19 July 2021).

[12] W. Pan, G. Ghoshal, C. Krumme, et al., Urban characteristics attributable to density-driven tie formation, Nature Commun. 4 (2013) 1961, http://dx.doi.org/10.1038/ncomms2961.

[13] B.F. Cardoso, S. Gonçalves, Universal scaling law for COVID-19 propagation in urban centers, 2020, http://dx.doi.org/10.1101/2020.06.22.20137604, medRxiv.

[14] R. Li, P. Richmond, B. Roehner, Effect of population density on epidemics, Physica A 510 (2018) 713–724, http://dx.doi.org/10.1016/j.physa.2018.07.025.

[15] H. Hu, K. Nigmatulina, P. Eckhoff, The scaling of contact rates with population density for the infectious disease models, Math. Biosci. 244 (2013) 125–134, http://dx.doi.org/10.1016/j.mbs.2013.04.013.

[16] J. Ottensmann, On population-weighted density, ERN: Other econometrics: Data collection & data estimation methodology (Topic), 2018, http://dx.doi.org/10.13140/RG.2.2.11789.44002.

[17] I.F. Mello, L. Squillante, G.O. Gomes, A.C. Seridonio, M. Souza, Epidemics, the ising-model and percolation theory: A comprehensive review focused on Covid-19, Physica A 573 (2021) 125963, http://dx.doi.org/10.1016/j.physa.2021.125963.

[18] A.M. Holdsworth, N.K.R. Kevlahan, D.J. Earn, Multifractal signatures of infectious diseases, J. R. Soc. Interface 9 (2012) 2167–2180, http://dx.doi.org/10.1098/rsif.2011.0886.

[19] X. Geng, F. Gerges, G.G. Katul, E. Bou-Zeid, H. Nassif, M.C. Boufadel, Population agglomeration is a harbinger of the spatial complexity of COVID-19, Chem. Eng. J. 420 (2021) 127702, http://dx.doi.org/10.1016/j.cej.2020.127702.
[20] A. Gowrisankar, L. Rondoni, S. Banerjee, Can India develop herd immunity against COVID-19? Eur. Phys. J. Plus 135 (2020) 1–9, http://dx.doi.org/10.1140/epjp/s13360-020-00531-4.
[21] J.W. Kantelhardt, Fractal and multifractal time series, in: Meyers R. (Ed.), Mathematics of Complexity and Dynamical Systems, Springer, New York, NY, 2012, http://dx.doi.org/10.1007/978-1-4614-1806-1_30.
[22] Y. Chen, J. Wang, Multifractal characterization of urban form and growth: the case of Beijing, Environ. Plan. B: Plann. Des. 40 (2013) 884–904, http://dx.doi.org/10.1068/b36155.
[23] P. Frankhauser, C. Tannier, G. Vuidel, H. Houot, An integrated multifractal modelling to urban and regional planning, Comput. Environ. Urban Syst. 67 (2018) 132–146, http://dx.doi.org/10.1016/j.compenvurbsys.2017.09.011.
[24] H. Salat, R. Murcio, E. Arcautea, Multifractal methodology, Physica A 473 (2017) 467–487, http://dx.doi.org/10.1016/j.physa.2017.01.041.
[25] A. Chhabra, R. Jensen, Direct determination of the $f(\alpha)$ singularity spectrum, Phys. Rev. Lett. 62 (1989) 1327–1330, http://dx.doi.org/10.1103/PhysRevLett.62.1327.
[26] S. Triambak, D.P. Mahapatra, A random walk Monte Carlo simulation study of COVID-19-like infection spread, Physica A 574 (2021) 126014, http://dx.doi.org/10.1016/j.physa.2021.126014.
[27] S. Chan, J. Chu, Y. Zhang, S. Nadarajah, Count regression models for COVID-19, Physica A 563 (2021) 125460, http://dx.doi.org/10.1016/j.physa.2020.125460.
[28] T. Lux, The social dynamics of COVID-19, Physica A 567 (2021) 125710, http://dx.doi.org/10.1016/j.physa.2020.125710.
[29] L.F.S. Scabini, L.C. Ribas, M.B. Neiva, A.G.B. Junior, A.J.F. Farfán, O.M. Bruno, Social interaction layers in complex networks for the dynamical epidemic modeling of COVID-19 in Brazil, Physica A 564 (2021) 125498, http://dx.doi.org/10.1016/j.physa.2020.125498.
[30] X. Li, On the multifractal analysis of air quality index time series before and during COVID-19 partial lockdown: A case study of Shanghai, China, Physica A 565 (2021) 125551, http://dx.doi.org/10.1016/j.physa.2020.125551.
[31] F. Bustamante-Castañeda, J.-G. Caputo, G. Cruz-Pacheco, A. Knippel, F. Mouatamide, Epidemic model on a network: Analysis and applications to COVID-19, Physica A 564 (2021) 125520, http://dx.doi.org/10.1016/j.physa.2020.125520.
[32] K.-B. Lee, S. Han, Y. Jeong, COVID-19, flattening the curve, and Benford's law, Phys. A: Stat. Mech. Appl. 559 (2020) 125090, http://dx.doi.org/10.1016/j.physa.2020.125090.
[33] P.M. Buscema, F.D. Torre, M. Breda, G. Massini, E. Grossi, COVID-19 in Italy and extreme data mining, Physica A 557 (2020) 124991, http://dx.doi.org/10.1016/j.physa.2020.124991.
[34] T. Odagaki, Exact properties of SIQR model for COVID-19, Physica A 564 (2021) 125564, http://dx.doi.org/10.1016/j.physa.2020.125564.